Spatial Mapping of the N-Dimensional Spectral Scatter Based on AVIRIS Data

Conrad M. Bielski[a]

[a]Jet Propulsion Laboratory, California Institute of Technology, 4800 Oak Grove Dr. (MS 171-B1), Pasadena, CA, 91109, USA – Conrad.M.Bielski@jpl.nasa.gov

Abstract – Imaging spectrometer data is data rich because it provides both fine spectral and spatial resolution information. The fine spectral resolution allows materials to be identified based on their spectral signature and is the driving force behind current information extraction techniques. These techniques require the identification of end-members, those extreme pixels making up the N-Dimensional spectral scatter. Recent experiments have shown that end-members change with changes in both spatial location and extent within a given scene which can affect pixel un-mixing techniques. On the other hand, understanding how end-members change based on their location and spatial association within a scene can also provide valuable information on the interaction and mixing of imaging spectrometer data pixels. The goal of this present research is to map the spectral end-member evolution spatially. This paper presents some initial results of shaving the spectrally extreme pixels from the N-dimensional spectral scatter.

Keywords: Imaging Spectroscopy, Pixel Purity Index, end-member selection, spectral un-mixing

INTRODUCTION

Imaging spectroscopy data provides images built up of contiguous and narrow spectral bands. Also known as hyperspectral remote sensing, present sensors are capable of resolving wavelengths ranging from the visible to the thermal infrared portions of the electromagnetic spectrum. As such, one can consider this type of imagery as both a blessing because airborne sensors such as the Airborne Visible and InfraRed Imaging Spectrometer (AVIRIS) provide users with fine spatial as well as spectral resolution imagery, as well as a curse because of the shear volume of data that needs to be processed.

Previous investigations into the selection of spectral end-members based on hyperspectral imagery showed that changing the location and/or the extent of an image over the same area modified the structure of the N-dimensional spectral scatter (Bielski 2003 a,b). This resulted in end-members having slightly different spectral signatures for the same general region. This motivated further study into the spatial/spectral relationship of hyperspectral imagery.

The generally accepted 'hourglass' approach to hyperspectral information extraction (Kruse 1999) primarily focuses on the spectral data. One of the key techniques in this approach to finding spectral end-members is the Pixel Purity Index (PPI) (Boardman et al. 1995). Essentially, this technique can be visualized as rolling the N-dimensional spectral scatter and recording every bump. The corners of this scatter will be the ones with the greatest number of hits and are considered to be the most spectrally extreme.

In this paper, the PPI idea was taken further by peeling off the extreme layers of the N-dimensional spectral scatter. The goal of this experiment was to better understand the evolution of the N-dimensional scatter with the ultimate goal of improving hyperspectral pixel un-mixing techniques. Furthermore, the relationships between the spectral layers being peeled and their spatial location were also shown. In the future, techniques that take advantage of the spatial component of hyperspectral data would also provide information that can be leveraged to improve segmentation and classification.

METHODOLOGY

The imagery used for this experiment was acquired by the AVIRIS instrument on July 23, 2002 over Cuprite, Nevada. It was acquired from an altitude of approximately 12 344 m above the target and resulted in a spatial resolution of approximately 12.5 m. A section of the flight line was selected over US route 95 with dimensions of 256 X 256 pixels.

First, the imagery was transformed to apparent reflectance using the ACORN atmospheric correction code. The water bands (bands 108-116, 153-169) and a few bands from each end of the spectrum (bands 1-3, 222-224) were taken out because of poor quality (noisy data). The remaining bands were used to compute the Minimum Noise Fraction (MNF) transform (ENVI 2002) in order to reduce the spectral dimensionality of the data set. The first 30 MNF bands were chosen from the resulting transform and applied to the experiment (figure 1).

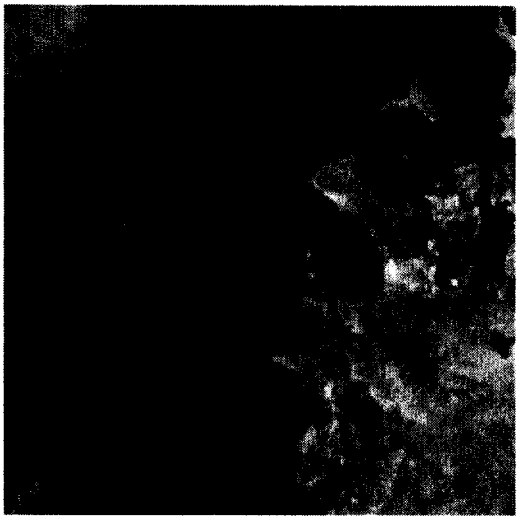

Figure 1 – MNF transform image showing bands 1 (red), 2 (green) and 3 (blue) for Cuprite, NV.

The next step was to peel the 30-dimensional MNF scatter layer by layer, where a layer was considered to be the extreme pixels of the N-dimensional scatter. A program was written

specifically for this purpose that repeatedly computed the PPI. A brief description of this program is described in figure 2. Each of the PPI results were based on 10 000 iterations.

1. Open MNF image file
2. Run PPI
3. Extract the top 100 purest pixels
4. Mask out the top 100 purest pixels
5. Open MNF file with masked pixels
6. Loop back to PPI until all pixels processed

Figure 2 – Description of the program developed to peel the extreme pixel layers from a spectral scatter.

RESULTS

The results of the program described in figure 2 were a series of purest pixels in the spectral sense based on the MNF data that ranged from the outside of the N-dimensional scatter inward. Unfortunately, the PPI library routine was unable to process the data after a certain point and therefore in this example only the first 102 layers were considered.

In figure 3, the spatial distribution of the purest pixels from each of the 102 layers is presented. In total, 10 548 extreme pixels were extracted from the image, which only makes up about 16% of the image. The linear feature going from top to bottom on the left side of the image (figure 3) that was almost entirely extracted as extreme spectral signatures was US route 95. The majority of the other locations that made up the 16% of the most extreme pixels of this particular scenes spectral distribution were generally clumped together. Without identifying the spectral signatures of the resulting pixels from each layer, it was difficult to visualize the evolution of the spectral signatures.

Since more than two dimensions are difficult to represent on paper, a pair of two dimensional scatter plots of the results are presented. The scatter plot in figure 4 clearly shows the influence that the first two MNF bands had on the computation of the PPI. This scatter plot with the 102 layers of pixels shown in different colours generally started from the outside of the scatter inward. A closer look at this figure also showed that some pixels within the scatter itself were also chosen as extremes of the 30-dimensional scatter (where the 30 dimensions are made up of the MNF bands). The scatter plot shown in figure 4 was different than the scatter plot shown in figure 5 which presented the last two MNF bands. The extreme spectral pixels tended to evolve from within this representation.

In table 1, the standard deviation of the first and last extreme pixel layer computed using the PPI are shown for the first 10 MNF bands. These results show a significant drop in the standard deviation between the first and last peeled layers. These results were not surprising because the goal of the PPI was to find the most spectrally extreme pixels. Such pixels will either be at the high or low end of the distribution and as the statistics indicated, there was a general decrease in the overall variability. However, these results do influence the PPI itself as can be seen in table 2 where the top 10 pixel counts from the 100 highest PPI results are shown for the first and final layer. The results for the PPI run on the 102 layer show that the surface of the 30-dimensional spectral scatter has been smoothed out compared to the original layer.

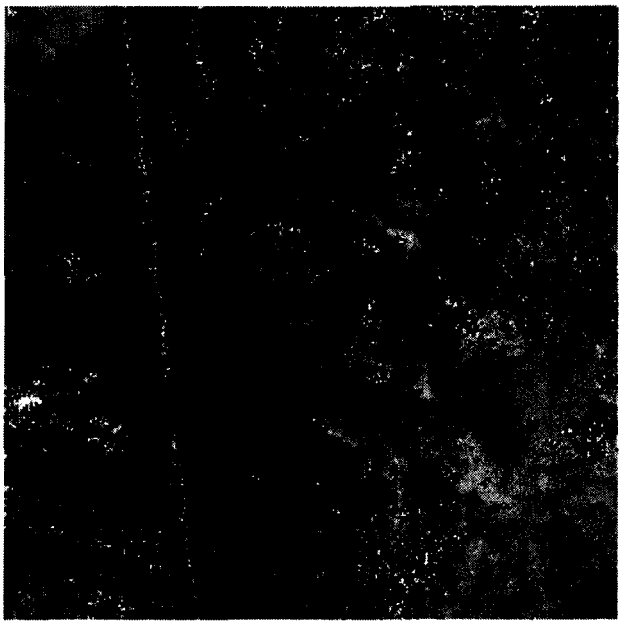

Figure 3 – The spatial locations of the extreme pixels shaved from 102 layers of the MNF scatter.

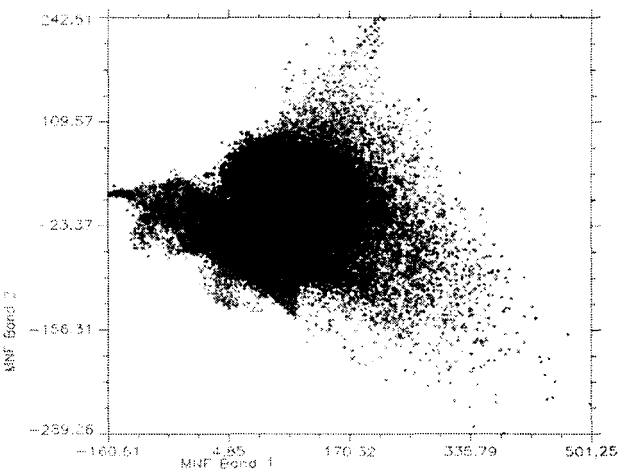

Figure 4 – Scatter plot of MNF bands 1 and 2 with the extreme pixels of the first 102 shaved layers overlaid in colour.

DISCUSSION

The above results are interesting but only paint a small portion of the picture because a mere 16% of the total pixels were processed. Furthermore, the extreme pixels themselves were grouped by layer rather than by spectral signature. This means that potentially different end-member spectra were grouped within the same PPI layer. As a result, the figures only showed how the pixel scatter layers evolved rather than how the end-member spectra evolved which is ultimately the goal that needs to be reached. More importantly, one would also like to know whether spectrally distinguishable regions can exist within the scatter itself and whether they are truly a mix of the spectrally extreme pixels that are normally found using the PPI. Future

questions that need to be investigated relate to spectral similarity and what kind of spectral mixing is occurring within a hyperspectral image. Both these questions are expected to be dealt with within the framework of this research in the future.

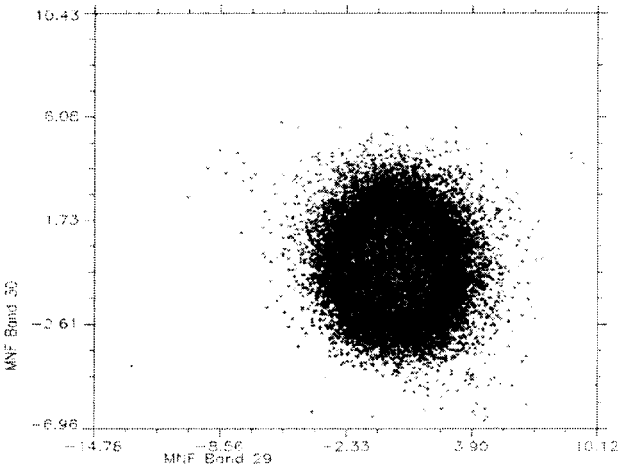

Figure 5 –Scatter plot of MNF bands 29 and 30 with the extreme pixels of the first 102 shaved layers overlaid in colour.

Table 1 – The standard deviation of the first 10 bands of the MNF image for the layers 1 and 102.

	Standard Deviation	
Band	Layer 1	Layer 102
1	222.00	106.40
2	131.70	47.96
3	44.95	25.24
4	75.54	24.33
5	41.68	21.84
6	30.26	18.21
7	37.32	19.20
8	28.23	12.11
9	21.66	8.03
10	19.99	8.01

Returning to figure 4, the scatter plot based on the first and second bands of the MNF transform provided a good visualization of what occurred when using the extreme pixel layer shaving routine (figure 2). The original shape of the scatter was irregular whereas if one took away all of the processed pixels (all the coloured pixels) the scatter becomes much more rounded. This has an effect on the algorithm that finds the spectrally extreme pixels and these effects are shown in table 1. The distribution of the number of total hits for the first iteration of the PPI was greatly skewed the right indicating that some pixels received a large number of hits compared to the distribution of the last iteration (table 2). This last iteration was less skewed because the total number of hits for the pixels considered to be spectrally extreme was evenly distributed.

Applying the 'hourglass' processing approach (Kruse 1999), the next step would be to visualize the pixels with the highest PPI in N-dimensional space in order to extract end-members for the scene in hand. With the range of extreme spectral pixels available to choose from at this point, the choice of a spectral end-member would be difficult. Furthermore, as the N-dimensional scatter is smoothed by more and more iterations, their distribution also changes as was shown above. This change in the total distribution has the effect of limiting or moderating potential end-members. As such, potential end-members would not be as dissimilar in spectral space making it more difficult to separate true end-members. Here, spatial location could provide the extra information required to decide on the final classes.

Table 2 – The number of hits (DN) for the top ten results out of 100 of the PPI for layers 1 and 102.

Layer 1		Layer 102	
DN	Npts	DN	Npts
1008	1	118	1
1032	1	119	4
1128	1	120	1
1164	1	121	1
1284	1	123	2
1320	1	125	1
1344	1	127	1
1356	1	128	1
1464	2	132	1
1608	1	141	1
3036	1	147	1

The center of gravity for the spectral scatter plot was not the mid-point between all sides in N-dimensions. Therefore shaving off the layers of extreme spectral pixels means that this center can be approached from a variety of directions and the core would be reached at different times from different directions. This has an implication in the next phase of this experiment where spectral similarity and direction will also be studied.

Note also that several pixels were identified as extreme that were located in the center of the first and second MNF band scatter plot (figure 4). These were most likely due to extreme spectra found in other MNF band combinations, however, further study is warranted again to explore their evolution both spectrally and spatially.

The US route 95 that was clearly delineated in figure 3 was almost entirely processed. With only 16% of total pixels processed, this indicated that the spectral signature of the road itself was found in a region of the 30-dimensional spectral scatter plot that was considered to be extreme. As such, one would also expect that this spectral end-member would not be a part of other spectral mixtures found within this scene.

Processed pixels to this point also had a tendency to clump together (figure 3). This clumping together in geographic space as well as spectral space indicates that materials that are close together are also spectrally similar. This is an important observation (also intuitive) because it also indicates that the notion of following the evolution of the N-dimensional spectral scatter to decompose it into it's spectral parts is a viable idea.

The expectation is that objects on the ground that are most spectrally unique will be found on the edges of the spectral scatter, whereas the pixels within the scatter will have a mixture of the spectrally pure end-members. This does not mean that the mixtures themselves cannot be identified as different materials. Subsequent research will try and show this possibility and requires a much more sophisticated approach.

The N-Dimensional simplex which is built based on spectral end-member selection and used for hyperspectral pixel un-mixing is very much dependent on what spectral signatures are chosen. A simplex must also encompass all possibilities which is why the chosen end-members must be extreme or 'pure' spectrally compared to the rest of the N-Dimensional distribution. If spectral end-members were chosen from within the distribution itself, a different model for pixel un-mixing will need to be developed.

CONCLUSIONS AND FUTURE WORK

This initial work showed the possibility of mapping the spectral signature from hyperspectral imagery to locations in space. It also provided insights into the evolution of the N-dimensional scatter plot based on an MNF transform of a measured hyperspectral scene of Cuprite, NV.

A routine that can entirely shave the N-dimensional spectral scatter will first be addressed. Subsequent research will focus on developing a spectral/spatial similarity index as well as an algorithm geared towards finding directional components of the spectral evolution of the N-dimensional scatter. In parallel, the need to identify classes automatically would also be advantageous and could be linked to other already developed spectral libraries.

References

Bielski, Conrad, M., 2003a, Space and End-member Selection. Talk given at the 2003 AVIRIS Workshop, Pasadena, California, February 25-28, 2003. Workshop paper will appear in proceedings

Bielski, Conrad, M., 2003b, The Influence of Spatial Extent on Endmember Selection in Imaging Spectrometer Data. Poster Presentation given at the Spectral Remote Sensing of Vegetation Conference, March 12-14, 2003, US Environmental Protection Agency, National Exposure Research Laboratory, Environmental Sciences Division, Las Vegas, Nevada.

Boardman, J.W., Kruse, F.A., and Green, R.O., 1995, Mapping target signatures via partial unmixing of AVIRIS data: in Summaries, Fifth JPL Airborne Earth Science Workshop, JPL Publication 95-1, v.1, pp. 23-26.

ENVI, 2002, ENVI User's Guide. ENVI Version 3.6, December 2002 edition, Research Systems Inc.

Kruse, F.A., Visible-Infrared Sensors and Case Studies, Chapter 11 in Remote Sensing for Earth Sciences: Manual of Remote Sensing, 3rd edition, Volume 3, edited by Andrew N. Rencz, 1999. John Wiley and Sons, Inc.

Acknowledgments

Funding for this project came from the National Research Council Associateship Program. Special thanks to Dr. Robert Green of the Jet Propulsion Laboratory, Pasadena, CA for his continued support of this project.